JCTC Journal of Chemical Theory and Computation

Strong Two-Photon Circular Dichroism in Helicenes: A Theoretical Investigation

Branislav Jansík

Teoretisk Kemi, Kemisk Institut, Aarhus Universitet, Langelandsgade 140, 8000 Aarhus C, Denmark

Antonio Rizzo*

Istituto per i Processi Chimico-Fisici del Consiglio Nazionale delle Ricerche (IPCF-CNR), Area della Ricerca, via G. Moruzzi 1, I-56124 Pisa, Italy

Hans Ågren

Theoretical Chemistry, School of Biotechnology, Royal Institute of Technology, Roslagstullsbacken 15, SE-10691 Stockholm, Sweden

Benoit Champagne

Laboratoire de Chimie Théorique Appliquée, FUNDP, Rue de Bruxelles 61, B-5000 Namur, Belgium

Received December 10, 2007

Abstract: Using a recently derived origin-invariant quadratic response approach combined with time-dependent density functional theory, four representative helicenes are shown to present a very strong two-photon circular dichroism (TPCD) response, which makes them candidates for the first experimental observation of a TPCD effect. The large response is attributed to the unique combination of chirality and electron delocalization. Comparison with electronic circular dichroism and two-photon absorption (TPA) shows that the three effects exhibit complementary features for unravelling the molecular structures. In particular, for the four (M)-helicenes studied here, the first, i.e., low-energy, dominant Cotton band is always negative, whereas for TPCD it is positive. From an analysis of the frontier orbitals describing most of the one-electron excitation vectors, the largest TPCD response of tetramethoxy-bisquinone-dithia-[7]-helicene has been attributed to the charge-transfer character of the excited state, like for the parent TPA effect. Moreover, the TPCD intensities are found to be mostly governed by the electric and magnetic dipole contributions, while the electric quadrupole terms are, on a relative basis, less important.

I. Introduction

Helicenes are fascinating compounds with unique chiro-optical properties. Like screws, strings, propellers, and other screw-shaped objects do in everyday life, helicenes and other helical systems, including DNA and proteins, play key roles at the molecular or supramolecular levels. Helicenes are made of ortho-fused aromatic rings and combine electron delocalization and helical conformation. The nonplanarity of the π-conjugated network and the associated chirality without stereogenic center results from steric hindrance, which already appears in [4]-helicene and leads to substantial optical

* Corresponding author phone: +39-050-315 2456; fax: +39-050-315 2442; e-mail: rizzo@ipcf.cnr.it.

10.1021/ct700329a CCC: $40.75
Published on Web 02/21/2008

rotation.[1] The first helicene to be obtained in nonracemic form was hexahelicene in 1955.[2] Since then, many homo- and heterohelicenes have been prepared, and synthetic routes have been improved to include functional groups while keeping enantiomeric excess.[3−18] Helicenes have been foreseen for a broad range of applications encompassing chiro-optical photoswitches,[19] enantioselective fluorescence detectors,[20] circularly polarized luminescence for back-lighting in liquid crystals displays,[21,22] or nonlinear optical (NLO) devices.[23,24] Theoretical investigations have been carried out to assess their structures, inversion pathways, aromatic character, and magnetic susceptibility as well as the oscillatory and rotatory strengths.[25−29] These studies further demonstrated that large second-order NLO responses (first hyperpolarizabilities) could be achieved by an appropriate choice of the position and nature of the substituents or by oxidation.[30−34] This unique combination of chirality and electron delocalization undoubtedly generates outstanding properties, including nonlinear circular dichroism, the subject of this paper.

The different interactions of the mirror images of helicenes with left- and right-circularly polarized light is fundamental in determining their handedness as well as to unravel other structural characteristics. More generally, structure-chiro-optics relationships are important for the qualitative and quantitative understanding of chirality, and helicenes appear as nice model compounds to address these features. Among the chiro-optical phenomena, the differential absorption associated with electronic and vibrational circular dichroisms [(E)CD and VCD] for electronic and vibrational transitions are well accepted approaches.[35] Then, vibrational Raman optical activity (VROA) spectroscopy, which probes differential Raman scattering, is receiving increased interest both experimental and theoretically to interpret spectral signatures.[36−39] Two-photon circular dichroism (TPCD)[40] is another chiral sensitive effect, whose interest has recently been revived thanks to the development of new theoretical approaches[41−43] combined with experimental detection improvements.[44] TPCD, the difference in two-photon absorption of left and right circularly polarized light, combines the advantages of two-photon absorption (TPA), i.e. 3D confocality and reduced frequency (and therefore f. ex. reduced damages to biological samples), with the fingerprinting capabilities of circular dichroism. Together with developments of improved measurement tools, progress in using TPCD requires the elaboration of theoretical schemes for simulating and interpreting the TPCD signatures. Since helicenes are among the systems that display the largest rotatory power and rotatory strengths, they turn out to be ideal candidates to study TPCD. In this work four helicenes have been selected (Figure 1) : the classical [6]-helicene (hexahelicene) and dithia-[7]-helicene and its tetramethoxy-bisquinone (TMB) derivative as well as tetrathia-[7]-helicene. For simplicity, only the left-handed enantiomers, known as (M)-helicenes, were considered. Their TPCD spectra are simulated and interpreted at the level of density functional theory (DFT). Key theoretical aspects are presented in section II, while section III describes the computational procedure. Results and Discussion found in section IV highlight the substantial TPCD signatures of helicenes, an incentive for experimental characterization.

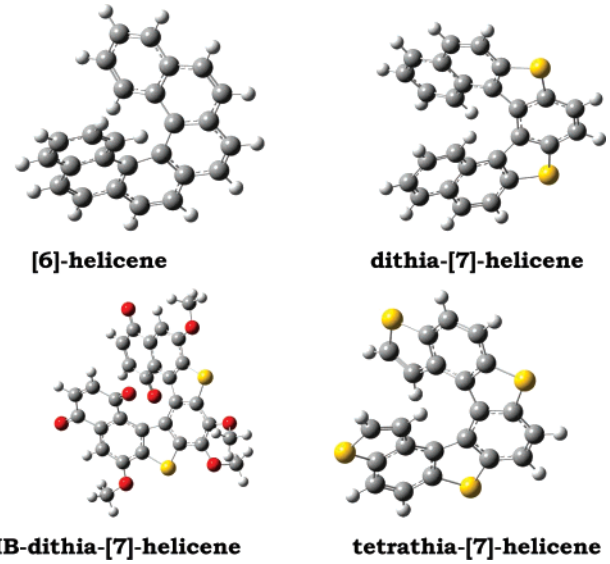

Figure 1. Sketch of the helicenes structures.

II. Theory

Two-photon circular dichroism arises from the difference in two-photon absorption of left (δ_L^{TP}) and right (δ_R^{TP}) circularly polarized light. δ indicates the two-photon absorption coefficient, and its CGS units are cm^4 s mol^{-1} $photon^{-1}$. The phenomenon, which is part of the vast area of high order optical activity, [45−49] has been theoretically described by Tinoco Jr.,[40] Power,[50] and Andrews[51] in the 1970s. In ref 41 we have given the definitions and discussed our computational approach to the ab initio determination of TPCD spectra. In ref 42 we presented a selection of origin invariant approaches, of which the one based on Tinoco's original formulation,[40] labeled as the "TI" approach, is employed in our present study. In ref 43 a comprehensive study of the ECD, TPA, and TPCD of all natural essential amino acids was carried out. In this section we therefore give only a brief outline the theory; for a detailed derivation we refer to refs 41 and 42.

Two-photon absorption circular dichroism is a differential effect observed when two photons (in our case, of equal frequency ω), one of which at least being of circular polarization, are absorbed inducing a transition from the initial state $|0\rangle$ to the final state $|f\rangle$ ($\hbar\omega_{0f} = 2\omega$ is the energy difference). The difference in absorption can be written, following the original expression of Tinoco Jr.,[40,42] as

$$\delta_L^{TP} - \delta_R^{TP} = \frac{4}{15}\frac{(2\pi)^2\omega^2 g(2\omega)N_A}{c_0^3(4\pi\epsilon_0)^2}\,{}^fR^{TP} \qquad (1)$$

$$\approx 4.67299 \times 10^{-32} \times \omega^2 g(2\omega) \times {}^fR^{TP} \qquad (2)$$

where ${}^fR^{TP}$ is the two-photon circular dichroism rotatory strength. In eq 1 $g(2\omega)$ is the normalized line shape, N_A is Avogadro's number, c_0 is the speed of light in vacuo, and ϵ_0 is the vacuum permittivity. Equation 2 yields the dichroism in CGS units from circular frequencies ω, line shapes $g(2\omega)$,

Table 1. Areas of the Portion of TPA, TPCD, and ECD Spectra Yielded by the First Six Excited States for the Four Helicenes Studied Here[a]

	TPA	TPCD × 1000	ECD
[6]-helicene	0.03	1.30 (0.30)	1.00 (−0.67)
dithia-[7]-helicene	0.58	2.27 (1.93)	0.50 (−0.30)
TMB-dithia-[7]-helicene	1.00	4.78 (2.22)	0.32 (−0.02)
tetrathia-[7]-helicene	0.56	2.90 (2.50)	0.51 (−0.15)

[a] Given relative to the area of the TPA spectrum of tetramethoxy-bisquinone (TMB) derivative of dithia-[7]-helicene (for TPA and TPCD) and to the (absolute) area of the ECD spectrum of hexahelicene (for ECD). For the CD spectra (TPCD and ECD) both the absolute area (obtained by integrating the absolute value of the spectral function over the whole set of frequencies) and (in parentheses) the actual area (with its sign, resulting from the balance of negative and positive portions of the spectrum) are given. Note that the relative area of the TPCD spectra is given in thousands of the reference unit. The calculations have been carried out at the TDDFT/B3LYP/aug-cc-pVDZ level of approximation.

and TPCD rotatory strengths ${}^fR^{TP}$ given in atomic units. When $\delta_L^{TP} - \delta_R^{TP}$ is computed in atomic units through eq 1, a multiplication by the conversion factor $\approx 1.89679 \times 10^{-50}$ yields the value in $cm^4\ s\ mol^{-1}\ photon^{-1}$. In ref 42 we have shown that the two-photon circular dichroism rotatory strength ${}^fR^{TP}$, in the particular formulation which we dubbed as the "TI" approach, is written as

$$ {}^fR^{TP} = -b_1 \mathscr{B}_1^{TI}(\omega) - b_2 \mathscr{B}_2^{TI}(\omega) - b_3 \mathscr{B}_3^{TI}(\omega) \tag{3} $$

$$ \mathscr{B}_1^{TI}(\omega) = \frac{1}{\omega^3} \sum_{\rho\sigma} M_{\rho\sigma}^{p,0f}(\omega) \mathscr{P}_{\rho\sigma}^{p,f0*}(\omega) \tag{4} $$

$$ \mathscr{B}_2^{TI}(\omega) = \frac{1}{2\omega^3} \sum_{\rho\sigma} \mathscr{T}_{\rho\sigma}^{+,0f}(\omega) \mathscr{P}_{\rho\sigma}^{p,f0*}(\omega) \tag{5} $$

$$ \mathscr{B}_3^{TI}(\omega) = \frac{1}{\omega^3} [\sum_{\rho} M_{\rho\rho}^{p,0f}(\omega)][\sum_{\sigma} \mathscr{P}_{\sigma\sigma}^{p,0f}(\omega)] \tag{6} $$

where the tensors $\mathscr{P}_{\alpha\beta}^{p,0f}(\omega_\beta)$, $M_{\alpha\beta}^{p,0f}(\omega_\beta)$, and $\mathscr{T}_{\alpha\beta}^{+,0f}(\omega_\beta)$ are defined through the following sum-over-states expressions (general case $\omega_\alpha + \omega_\beta = \omega_{0f}$)

$$ \mathscr{P}_{\alpha\beta}^{p,0f}(\omega_\beta) = \frac{1}{\hbar} \sum_P \sum_{n\neq 0} \frac{(\mu_\alpha^p)^{0n}(\mu_\beta^p)^{nf}}{\omega_\alpha - \omega_{0n}} \tag{7} $$

$$ M_{\alpha\beta}^{p,0f}(\omega_\beta) = \frac{1}{\hbar} \sum_P \sum_{n\neq 0} \frac{(\mu_\alpha^p)^{0n}(m_\beta)^{nf}}{\omega_\alpha - \omega_{0n}} \tag{8} $$

$$ \mathscr{T}_{\alpha\beta}^{+,0f}(\omega_\beta) = \frac{1}{\hbar} \epsilon_{\beta\rho\sigma} \sum_P \sum_{n\neq 0} \frac{(T_{\alpha\rho}^{+})^{0n}(\mu_\sigma^p)^{nf}}{\omega_\alpha - \omega_{0n}} \tag{9} $$

P takes care of the permutation of the couples (operator/associated frequency), whereas the Levi-Civita $\epsilon_{\beta\rho\sigma}$ tensor in eq 9 implies Einstein summation over repeated indices (ρ and σ). The parameters b_1, b_2, and b_3 in eq 3 depend on the polarization and propagation status of the beam, and they are tabulated for a few combinations in Table 2 of ref 40. Also, the notation $(X_\alpha)^{0n}$ indicates the matrix element $< 0 \mid X_\alpha \mid n >$ of the α Cartesian component of the operator X between the ground $\mid 0 >$ and excited $\mid n >$ electronic states. The operators X appearing in the infinite summations are the velocity operator μ^p

$$ \mu_\alpha^p = \sum_i \frac{q_i}{m_i} p_{i\alpha} \tag{10} $$

involving a sum over the linear momentum p_i of all particles of mass m_i and charge q_i; the magnetic dipole operator m

$$ m_\alpha = \sum_i \frac{q_i}{2m_i} l_{i\alpha} = \sum_i \frac{q_i}{2m_i} (r_i \times p_i)_\alpha \tag{11} $$

involving the position r_i and angular momentum l_i operators; and the mixed length-velocity form of the quadrupole operator ($T_{\alpha\beta}^{+}$), defined as

$$ T_{\alpha\beta}^{+} = \sum_i \frac{q_i}{m_i} (p_{i\alpha} r_{i\beta} + r_{i\alpha} p_{i\beta}) \tag{12} $$

Equation 3, the "TI" equation, can be proven to yield origin invariant results for the observable—the circular dichroism—independent of the completeness of the one-electron basis set employed in the calculation.[42] To end this section we recall that the TPCD rotational strength ${}^fR^{TP}$ is a quantity analogous to the ordinary ECD rotatory strength[52,53] ${}^fR$

$$ {}^fR = \frac{3}{4} \mathscr{T}[\langle 0 \mid \hat{\mu} \mid f\rangle \cdot \langle f \mid \hat{m} \mid 0\rangle] \tag{13} $$

which enters the expression of the linear circular dichroism (written here in terms of the anisotropy of the molar absorptivity ϵ)

$$ \Delta\epsilon = \epsilon_L - \epsilon_R = \frac{64\pi^2 \omega g(\omega) N_A}{9 \times 1000 \times \ln(10) \times (4\pi\epsilon_0) \times \hbar c_0^{\,2}} \times {}^fR \tag{14} $$

$$ \approx 2.73719 \times 10^{-2} \times \omega g(\omega) \times {}^fR \tag{15} $$

Equation 15 gives $\Delta\epsilon$ in the usual units of $dm^3\ mol^{-1}\ cm^{-1}$ when, as for eq 2, ω and the rotatory strength ${}^fR$ are in atomic units. Moreover, in the dipole approximation the expression of the two-photon absorption for two photons of equal frequency reads usually as[40,54]

$$ \delta^{TP} = \frac{(2\pi)^2 \omega^2 g(2\omega) N_A}{c_0^{\,2}(4\pi\epsilon_0)^2} \frac{1}{30} \{F[\sum_\rho S_{\rho\rho}^{0f}(\omega)]^2 + (G+H)(\sum_{\rho\sigma} S_{\rho\sigma}^{0f}(\omega) S_{\rho\sigma}^{0f}(\omega))\} $$

$$ = \frac{(2\pi)^2 \omega^2 g(2\omega) N_A}{c_0^{\,2}(4\pi\epsilon_0)^2} \frac{1}{30} \bar{\delta} \tag{16} $$

$$ \approx 8.00460 \times 10^{-31} \times \omega^2 g(\omega) \times \bar{\delta} \tag{17} $$

where the $S_{\alpha\beta}^{0f}(\omega_\beta)$ tensor elements given by

Table 2. Excitation Energy $\hbar\omega_{0n}$ (eV), Wavelength λ (nm), Parameters $\mathscr{B}_1^{TI}$ (Eq 4), $\mathscr{B}_2^{TI}$ (Eq 5), and $\mathscr{B}_3^{TI}$ (Eq 6), and Rotational Strengths ${}^fR^{TP}$ (Eq 3), $\bar{\delta}$ (Eq 16), and ${}^fR$ (Eq 13) for Each of the Six Lowest Excited States of the Four Helicenes Studied Here at the TDDFT/B3LYP/aug-cc-pVDZ Level of Approximation[a]

	state (n)	$\hbar\omega_{0n}$ (eV)	λ (nm)	B_1^{TI}	B_2^{TI}	B_3^{TI}	${}^fR^{TP}$	$\bar{\delta}$	$10^3 \times {}^fR$
[6]-helicene[b]	1	3.20	387.1	−536	84	0	3046	572	0.7
	2	3.36	369.5	97	46	−231	−1135	999	4.5
	3	3.62	342.2	−28	1	0	168	1355	−1073.8
	4	3.72	333.3	0	−71	−260	−376	1854	149.3
	5	3.84	323.0	−5	−18	0	65	1270	−109.7
	6	3.93	315.8	50	7	−109	−534	1123	82.6
dithia-[7]-helicene	1	3.14	395.4	15	28	0	−144	2650	−151.2
	2	3.31	374.3	42	−1	481	713	883	115.2
	3	3.65	339.7	−1882	−43	−2331	6719	80475	26.0
	4	3.81	325.2	31	−88	−210	−427	4903	−43.0
	5	3.85	321.7	12	28	0	−130	491	−364.5
	6	3.98	311.6	−204	27	0	1167	49478	−5.2
TMB-dithia-[7]-helicene	1	2.03	610.9	311	−65	890	42	5152	2.5
	2	2.18	568.4	−2326	−155	0	14265	105094	−201.0
	3	2.29	540.8	287	−62	0	−1599	4324	41.7
	4	2.48	499.9	51	7	0	−319	49462	56.3
	5	2.50	495.4	−497	−164	−2168	−1030	47714	−44.0
	6	2.64	469.5	333	25	−120	−2291	27047	115.9
tetrathia−[7]−helicene	1	3.22	384.9	−258	−43	−89	1456	1260	116.6
	2	3.22	384.8	13	−11	0	−56	2417	−276.5
	3	3.78	327.6	148	−68	0	−752	34356	−149.8
	4	3.81	325.5	−1934	354	−2314	6267	65678	−2.8
	5	4.06	305.7	−60	30	0	301	9970	−40.7
	6	4.09	302.8	−650	−54	−499	3014	20138	133.9

[a] The TPA strength and the TPCD rotational strength has been computed for two circularly polarized photons ($b_1 = G + H = 6$, $b_2 = -b_3 = F = 2$). Atomic units where not explicitly specified. [b] For the five lowest lying excitation energies (nm) and corresponding rotational strengths ${}^fR$ ($\times 10^3$ au, in parentheses) Furche et al.[27] computed (at the TDDFT level, using the BP86 XC functional and with an SV(P)+ basis set): 411. (−2.); 395. (6.); 365. (−457.); 364. (87.); 358. (−291.). The experimental values taken from ref 68 and referring to the measurements of ref 69 are as follows: 412. (2.5); 347. (−137.); 325. (−393.); 292. (−17); 244. (609.). Note that, besides the conversion of units, the rotational strengths taken from refs 27 and 68 are multiplied here by the factor 3/4, which makes them consistent with the convention used in eq 13.

$$S_{\alpha\beta}^{0f}(\omega_\beta) = \frac{1}{\hbar}\sum_P \sum_{n\neq 0} \frac{(\mu_\alpha)^{0n}(\mu_\beta)^{nf}}{\omega_\alpha - \omega_{0n}} \tag{18}$$

are related to those of the $\mathscr{P}_{\alpha\beta}^{p,0f}(\omega_\beta)$ tensor in the limit of a complete one-electron basis set by the relationship

$$\mathscr{P}_{\alpha\beta}^{p,0f}(\omega_\beta) = -\omega_\alpha{}^2 S_{\alpha\beta}^{0f}(\omega_\beta) \tag{19}$$

but are defined using the traditional electric dipole moment operator, μ

$$\mu_\alpha = \sum_i q_i r_{i\alpha} \tag{20}$$

As b_1, b_2, and b_3, see above, the F, G, and H parameters take different values for different polarization and propagation conditions of the two photons. Note that the following relationship holds (cf. eqs 1 and 16 above)

$$\frac{\delta_L^{TP} - \delta_R^{TP}}{\delta^{TP}} = \frac{8}{c_0}\frac{{}^fR^{TP}}{\bar{\delta}} \tag{21}$$

Again, eq 17 above can be used to obtain the TPA rate in the absolute units of $cm^4\ s\ mol^{-1}\ photon^{-1}$ from all quantities involved—ω, $g(2\omega)$, and $\bar{\delta}$—given in atomic units.

III. Computational Details

The computational schemes employed for the calculation of TPCD, TPA, and ECD have been elaborated and detailed in refs 41 and 42. As shown in ref 41, two-photon circular dichroism can be evaluated via analytical response theory, in a formulation where the summation over intermediate states is replaced by the solution of linear equations, without explicit knowledge of the excited-state wave functions. As a consequence, the properties of interest are obtained in a size-extensive manner, whenever the computational model is itself size-extensive. In the present case, time-dependent density functional theory (TDDFT) with frequency dependent quadratic response theory where both the density and its response are computed employing the B3LYP exchange-correlation functional[55−58] is employed to model TPA and TPCD.

We have calculated the one- and two-photon circular dichroism spectra and the two-photon absorption spectra for the six lowest excited states $|f>$ of the four helicenes. Their structure is shown in Figure 1. The calculations involved neutral, gas-phase, molecules. Note that, with respect to ref 10, the dodecyloxy groups were replaced by methoxy groups in order to reduce the computational cost with only a minor impact on the electronic structure and properties of the helicene. The molecular geometry was taken from B3LYP/6-31G* optimization. The six excited states energies ω_{0f} were obtained from the poles of a linear response function.[59] The two-photon circular dichroism rotatory strength ${}^fR^{TP}$ was calculated within the "TI" formulation defined in ref 42 and

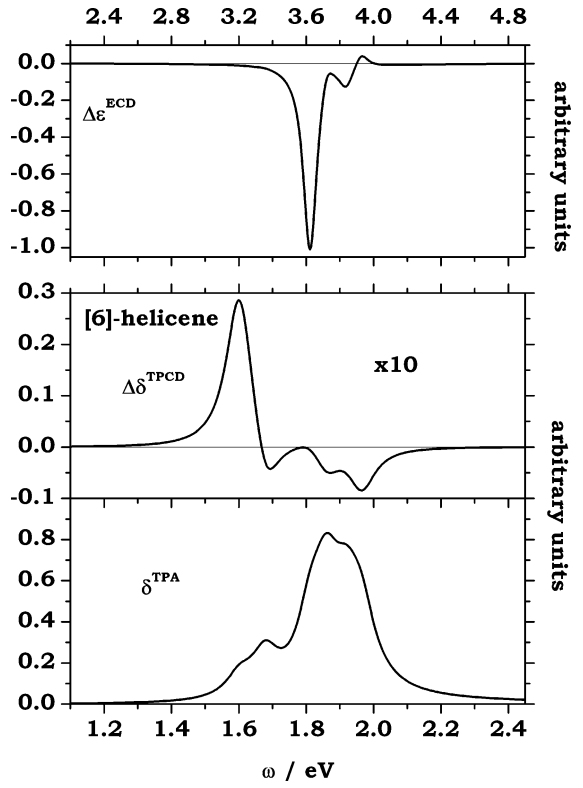

Figure 2. ECD, TPCD, and TPA spectra obtained at the DFT/B3LYP/aug-cc-pVDZ level arising from the lowest six excited electronic states for [6]-helicene.

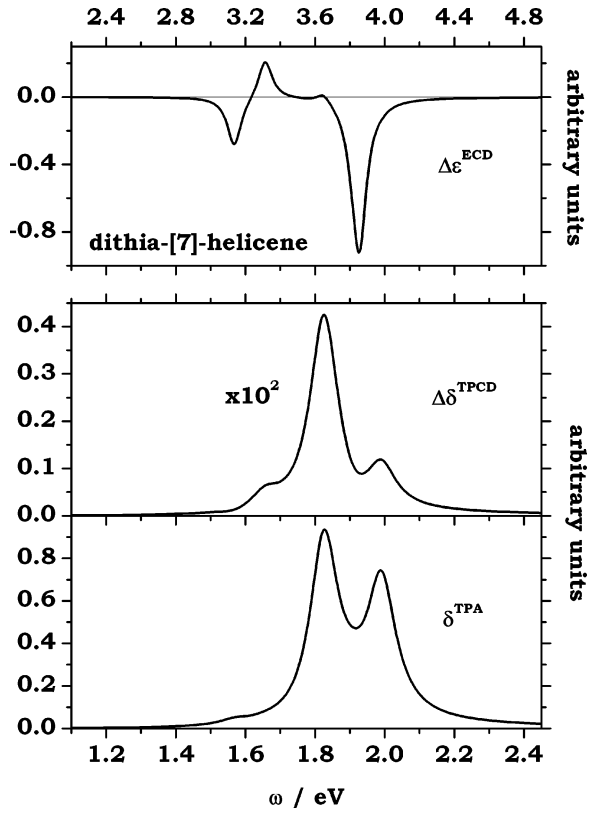

Figure 3. ECD, TPCD, and TPA spectra obtained at the DFT/B3LYP/aug-cc-pVDZ level arising from the lowest six excited electronic states for dithia-[7]-helicene.

briefly outlined in eqs 3−9 above. The $\mathscr{P}^{p,0f}_{\alpha\beta}(\omega_\beta)$, $M^{p,0f}_{\alpha\beta}(\omega_\beta)$, and $\mathscr{T}^{+,0f}_{\alpha\beta}(\omega_\beta)$ tensors were then evaluated as single residues of the appropriate quadratic response functions within the response theory framework, for each final excited state $|f>$ at the frequency $\omega = \omega_{0f}/2$, adopting the procedure described in ref 43 to ensure that phase factors were all properly taken into account. As stated above, all the property calculations were performed employing the B3LYP exchange-correlation functional.[55−57] The aug-cc-pVDZ basis set[60] was used throughout.

Both the absorption and circular dichroism spectra presented here were obtained, according to eqs 16, 14 and 1, assuming a Lorentzian as line shape function—$g(n\omega)$, n = 1,2—with a full width at half-maximum Γ of 0.1 eV and with maxima determined so that each Lorentzian, when integration is performed over the whole frequency spectrum, yields the value of the TPA strength ($\bar{\delta}$), TPCD ($^fR^{TP}$), or ECD (^fR) rotational strength for the given excited state. A Γ of 0.1 eV appears to be a reasonable assumption, considering current spectroscopic spectral resolution capabilities. It is to be noted that the spectral profile may change quite heavily as the value of Γ is varied. The results shown and discussed in the following for the two-photon processes correspond to an experimental setup with two left circularly polarized beams of equal frequency propagating parallel to each other. For this arrangement, $F = -2$, $G + H = 6$, $b_1 = 6$, and $b_2 = -b_3 = 2$.[40]

The intensities of the two-photon spectra presented in the next section are of arbitrary units and normalized in each figure to the area of the two-photon absorption spectrum, thus allowing for an absolute comparison of the TPA and TPCD spectra. For this purpose the prefactor in eq 21, see also ref 41, was included into the scaling of the TPCD spectra. The ECD spectra, obtained applying eq 14 are also given in arbitrary units.

All calculations were carried out using a parallel version of the DALTON 2.0 electronic structure program.[61]

IV. Results and Discussion

TMB-dithia-[7]-helicene appears to be the strongest two-photon absorber within our selection of helicenes, see Table 1, 1−2 orders of magnitude more effective than[6]-helicene and approximately twice as strong as the di- and tetrathia-[7]-helicenes. It is also the most efficient in dichroic response, with its TPCD spectrum covering, in the range of frequencies chosen here, ca. 4.8‰ of its TPA response. These features can be associated with the presence of symmetric substitutions by donors and acceptors.[62−67] The ratios between the TPCD and TPA areas are thus slightly larger for these helicenes than for the amino acids studied in refs 41 and 43, where they amount to up to 2−5‰. Note however the extremely favorable TPCD/TPA ratio in the case of [6]-helicene, where the absolute area of the TPCD spectra is only a factor of ≈30 smaller than that of the corresponding TPA spectrum as a result of its smaller TPA response compared to the other helicenes. [6]-Helicene appears to be the most efficient in the linear dichroism response, its ECD spectrum covering an area ca. twice that of the di- and tetrathia-[7]-helicenes and ca. three times that of the tetramethoxy-

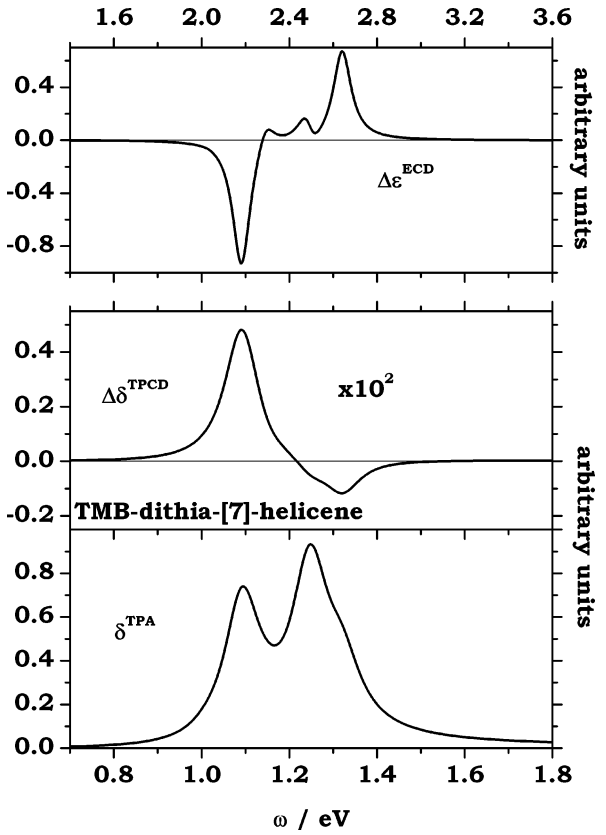

Figure 4. ECD, TPCD, and TPA spectra obtained at the DFT/B3LYP/aug-cc-pVDZ level arising from the lowest six excited electronic states for TMB-dithia-[7]-helicene.

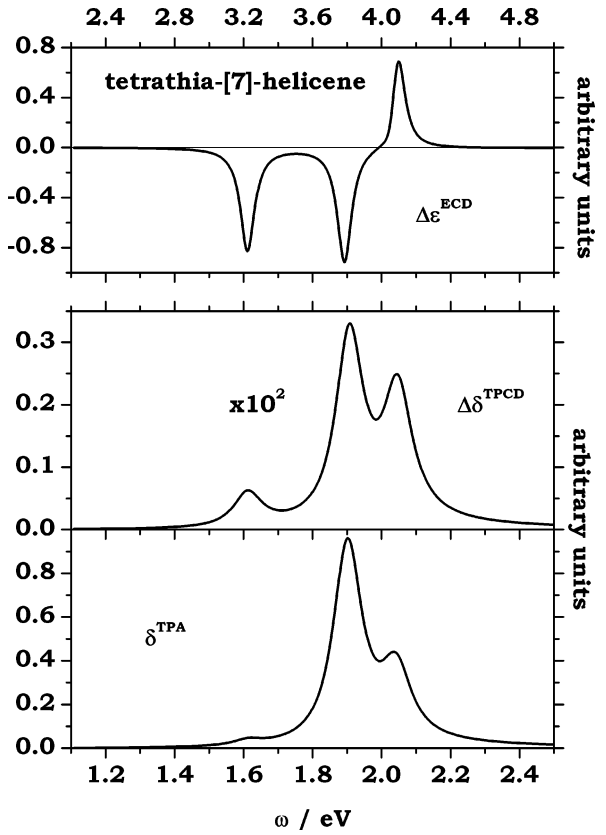

Figure 5. ECD, TPCD, and TPA spectra obtained at the DFT/B3LYP/aug-cc-pVDZ level arising from the lowest six excited electronic states for tetrathia-[7]-helicene.

bisquinone derivative. The largest ECD intensity obtained by integrating the area of the peaks is therefore found for the homohelicene, and it decreases with the number of thiophene rings or with the substituents.

Rotational strengths and spectral characteristics are listed in Table 2, whereas the spectra are displayed in Figures 2−5. From the data in Table 2, with the help of eqs 2, 15, and 17, the spectroscopic properties (TPCD, ECD and TPA rates, respectively) can be obtained in the commonly employed absolute units. Figure 6 shows comparison between our ECD simulated spectra and experiment. Note that, where available, experiment is performed in solution (see caption for details), and the corresponding spectra are reported without further elaboration, with the form and units given in the original references. Our data are given as $\Delta\epsilon$ in the usual units of $dm^3\ mol^{-1}\ cm^{-1}$. It is beyond the scope of this study to comment in detail on the individual features of the experimental vs our isolated molecule approximation spectra or to speculate on the effect of intermolecular interactions in solution for ECD. Figure 6 should therefore only be intended to provide support to the very general and concise comments given in the following paragraphs.

The four helicenes exhibit excited states with substantial ${}^fR^{TP}$ values, more than 1 order of magnitude larger than for any of the essential proteinogenic amino acids of refs 41 and 43. For instance, ${}^fR^{TP}$for the second excited-state of TMB-dithia-[7]-helicene amounts to more than 14 000 au. As for the ECD intensities, these large chiro-optical responses result from the fact that the π-conjugated electron network is associated with chirality.[1]

In fact, see also refs 27 and 28, the TDDFT approach generally underestimates the excitation energies, though to a lesser extent when using the B3LYP exchange-correlation functional since it contains 20% of exact Hartree−Fock exchange. For [6]-helicene, our TDDFT results are in agreement with the TDDFT data of ref 27 where the main low-energy band is shown to be associated with the 2^1B excited state. On the other hand, with respect to experiment, a blue-shift has to be applied to match the spectra. For TMB-dithia-[7]-helicene the simulated ECD spectrum, which exhibits a negative Cotton effect at a rather large wavelength (568 nm) followed by a small and then a large positive band, also reproduces the sign alternation of the Cotton effects observed in the experimental spectrum,[10] recorded for a dilute solution to avoid the formation of aggregates. Differences of shapes between the simulated and experimental spectra originate from the absence of vibronic treatment of our simulation. Yamada et al.[5] reported the ECD spectrum of tetrathia-[7]-helicene. With the exception of the near degeneracy of the two first transitions, which does not allow for the reproduction of the positive experimentally observed Cotton effect of the lowest-energy excitation, the agreement is also good. Finally, to our knowledge, the experimental ECD spectrum of dithia-[7]-helicene is not known. In these left-handed helicenes, the lowest-energy dominant band always displays a global negative Cotton effect. On the other hand, for the same helicenes, the global TPCD signal due to the six lowest-

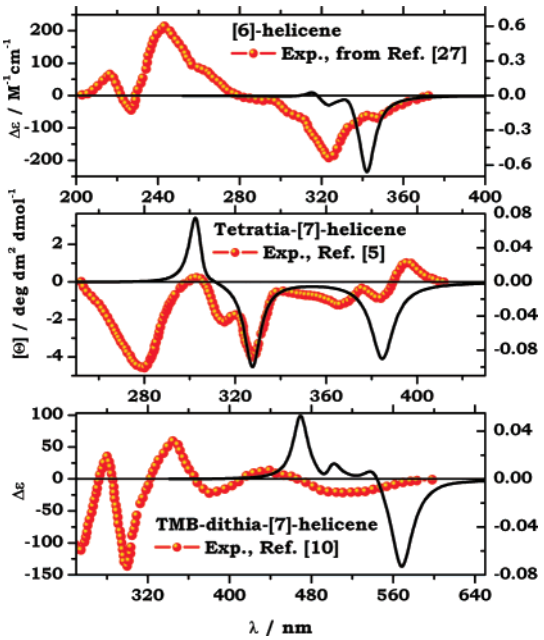

Figure 6. Comparison between experimental and simulated ECD spectra for three of the helicenes studied here. Our spectra, ordinates on the right, show $\Delta\epsilon$ in units of dm^3 mol^{-1} cm^{-1}. Experiment (ordinate on the left) is given in the form and units found in the original papers. In particular: a) for [6]-helicene the spectrum is taken from Figure 5 of ref 27, it comes originally from ref 69 (see also ref 68), and it was taken in a methanol solution; b) for tetrathia-[7]-helicene we report the spectrum found in Figure 2 of ref 5, taken in solution of chloroform; and c) for TMB-dithia-[7]-helicene we refer to Figure 1 of ref 10, in particular to the one recorded on a 2×10^{-5} M solution of tetradodecyloxy-helice-bisquinone in dodecane. Note a change of sign with respect to the spectrum in ref 10, which was taken on the P-helicene.

energy excitations is positive, see Table 1, and the first, i.e., low-energy, dominant band is always positive. In the dithia- and tetrathia-[7]-helicene the TPCD profile is positive over the low-excitation energy window, with our choice of line shape width Γ of 0.1 eV (ca 800 cm^{-1}). On the other hand, for the two other compounds, a first positive band at lowest energy is followed by a negative pattern. Summarizing this analysis, ECD and TPCD bring complementary chiro-optical information on the helicenes, a neat example of how nonlinear spectroscopies probe aspects of chirality which are different from those yielded by linear spectroscopies.[70]

The TPA spectra display essentially two major peaks. Their relative intensities change from one compound to another. In particular, the relative intensity of the lowest energy band with respect to the intensity of the second band increases as the number of thiophene rings increases.

The largest contributions to ${}^fR^{TP}$ come from the $\mathscr{B}_1^{TI}$ and $\mathscr{B}_3^{TI}$ terms, demonstrating the lesser importance of the electric quadrupole terms with respect to the magnetic dipole terms. This substantiates partly the general assumption on the negligible amplitude of the electric quadrupolar effects with respect to the magnetic dipole contributions.[71] On the other hand, the relative importance of the two dominant magnetic dipole terms—as well as their signs—depend much on the excited-state, and no consistent pattern could be pinpointed from Table 2.

Tables 3−6 list the major contributions to the excitation vectors of the lowest six excited states of each helicene, while selected MOs are shown in Figure 7. For all excited states of interest in the tables only coefficients of absolute value larger than 0.2 are reported, whereas the coefficients corre-

Table 3. Largest Contributions to the Excitation Vectors for the Lowest Six Excited States of [6]-Helicene[a]

state (n)	$\hbar\omega_{0n}$ (eV)	excitation		coefficient
1	3.20	HOMO−1	LUMO	−0.510
		HOMO	LUMO+1	−0.476
2	3.36	HOMO−1	LUMO+1	0.338
		HOMO	LUMO	−0.616
3	3.62	HOMO−1	LUMO	−0.465
		HOMO	LUMO+1	0.507
4	3.72	HOMO−3	LUMO	0.307
		HOMO−1	LUMO+1	0.510
		HOMO	LUMO	0.292
5	3.84	HOMO−2	LUMO	0.684
6	3.93	HOMO−3	LUMO	0.322
		HOMO−2	LUMO+1	−0.380
		HOMO−1	LUMO+1	−0.306
		HOMO	LUMO+3	−0.294

[a] In terms of single excitations between the molecular orbitals depicted in Figure 6. Atomic units where not explicitly specified.

Table 4. Largest Contributions to the Excitation Vectors for the Lowest Six Excited States of Dithia-[7]-helicene[a]

state (n)	$\hbar\omega_{0n}$ (eV)	excitation		coefficient
1	3.14	HOMO	LUMO	−0.697
2	3.31	HOMO−1	LUMO	0.671
3	3.65	HOMO−2	LUMO	−0.536
		HOMO	LUMO+1	0.446
4	3.81	HOMO−2	LUMO	−0.426
		HOMO	LUMO+1	−0.534
5	3.85	HOMO−3	LUMO	−0.387
		HOMO−1	LUMO+1	0.520
6	3.98	HOMO−3	LUMO	0.541
		HOMO−1	LUMO+1	0.442

[a] In terms of single excitations between the molecular orbitals depicted in Figure 6. Atomic units where not explicitly specified.

Table 5. Largest Contributions to the Excitation Vectors for the Lowest Six Excited States of TMB-dithia-[7]-helicene[a]

state (n)	$\hbar\omega_{0n}$ (eV)	excitation		coefficient
1	2.03	HOMO	LUMO	0.700
2	2.18	HOMO−1	LUMO	−0.685
3	2.29	HOMO	LUMO+1	0.702
4	2.48	HOMO−4	LUMO	0.283
		HOMO−2	LUMO	−0.594
5	2.50	HOMO−1	LUMO+1	0.625
6	2.64	HOMO−6	LUMO	0.379
		HOMO−5	LUMO	0.306
		HOMO−4	LUMO+1	−0.276
		HOMO−2	LUMO+1	0.237
		HOMO−1	LUMO+1	0.303

[a] In terms of single excitations between the molecular orbitals depicted in Figure 6. Atomic units where not explicitly specified.

Table 6. Largest Contributions to the Excitation Vectors for the Lowest Six Excited States of Tetrathia-[7]-helicene[a]

state (n)	$\hbar\omega_{0n}$ (eV)	excitation		coefficient
1	3.22	HOMO−1	LUMO	0.686
2	3.22	HOMO	LUMO	−0.700
3	3.78	HOMO−2	LUMO	−0.681
4	3.81	HOMO−3	LUMO	0.668
		HOMO	LUMO+1	0.208
5	4.06	HOMO−1	LUMO+1	0.641
		HOMO	LUMO+2	0.267
6	4.09	HOMO−1	LUMO+2	0.231
		HOMO	LUMO+1	−0.618

[a] In terms of single excitations between the molecular orbitals depicted in Figure 6. Atomic units where not explicitly specified.

sponding to de-excitations in the paired structure of the excitation vectors[59,72] are neglected. In the case of [6]-helicene, two different and almost "opposite" (in sign) combinations of HOMO − 1 → LUMO and HOMO → LUMO + 1 excitations are responsible for both the dominant bands in ECD and TPCD. Indeed, the first combination leads to the TPCD strong absorbing state at 3.20 eV ($^fR^{TP} = 3046$ au), whereas the second combination yields the ECD intense state at 3.62 eV ($^fR = -675$ au). This is another evidence of the fact that ECD and TPCD are governed by different mechanisms. In the case of dithia-[7]-helicene and tetrathia-[7]-helicene the characters—and therefore the ECD, TPA, and TPCD amplitudes and signs—of the two first transitions are inverted. In dithia-[7]-helicene the first band at 3.14 eV is described by a HOMO → LUMO transition, while the HOMO − 1 → LUMO single excitation governs the second excited state (3.31 eV). Then, for tetrathia-[7]-helicene, as a result of the presence of two additional thiophene rings, the two first transitions are almost degenerate and have excitation energies of 3.22 eV. Nevertheless, the corresponding excited states keep distinct characters as shown by their singly excited determinant vectors. For these thiophene-containing helicenes, the most intense TPCD band, corresponding to the third excited state at 3.65 eV for dithia-[7]-helicene and to the fourth excited state at 3.81 eV for tetrathia-[7]-helicene, see Table 2, are related to HOMO − 2 → LUMO (dithia-[7]-helicene) and HOMO − 3 → LUMO (tetrathia-[7]-helicene) transitions. These dominant TPCD excitations have in fact similar character since the HOMO − 2 of dithia-[7]-helicene and the HOMO − 3 of tetrathia-[7]-helicene look alike, i.e., present much similarities in their nodal structures, see Figure 7. The most ECD-intense excited states are instead the fifth (at 3.85 eV) for the dithia and the second (at 3.22 eV) for the tetrathia-[7]-helicenes. The former is essentially the result of the combination of HOMO − 3 → LUMO and HOMO − 1 → LUMO + 1 transitions, whereas the latter is essentially a clean HOMO → LUMO transition. In the case of the substituted helicene, the strong ECD and TPCD signals are both associated with the second excited state at 2.18 eV, which is mostly described as a HOMO − 1 → LUMO transition. The MOs of the TMB-dithia-[7]-helicene are different from those of the other helicenes, where the frontier orbitals are delocalized over the whole systems. Indeed, the LUMO is localized on the terminal quinone groups, whereas the HOMO − 1 is localized on the thiophene and benzene rings, demonstrating the charge-transfer character of the transition.

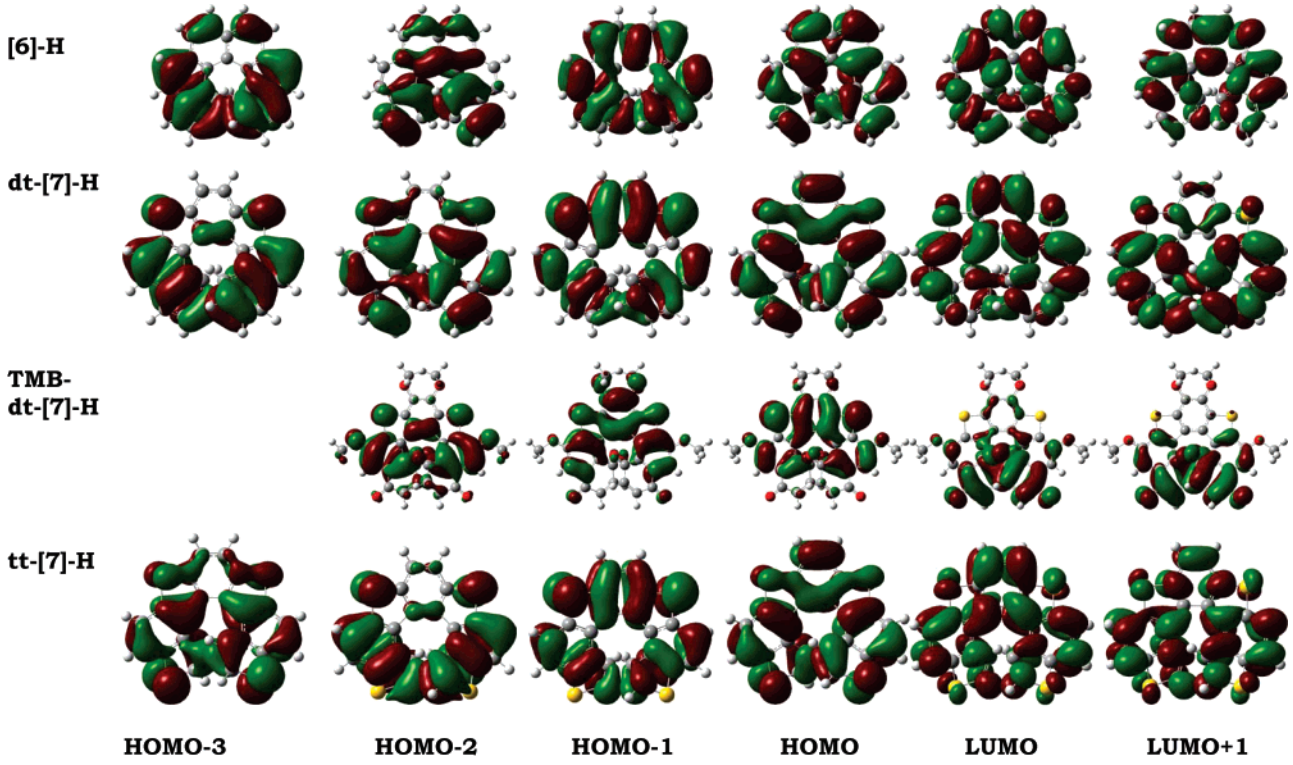

Figure 7. The relevant molecular orbitals of [6]-helicene, dithia-[7]-helicene, TMB-dithia-[7]-helicene, and tetrathia-[7]-helicene, obtained at the B3LYP/aug-cc-pVDZ level.

Conclusions

Using a recently derived origin-invariant quadratic response approach combined with time-dependent density functional theory, here it was demonstrated that helicenes present a strong two-photon circular dichroism (TPCD) response, which makes them candidates for a first experimental observation of TPCD. Indeed the $\Delta\delta^{TPCD}/\bar{\delta}$ ratio amounts to a few per mil, close to the detection limit estimated in ref 44. In that reference Markowitz and co-workers have discussed modified Z-scan techniques which the authors claim should be able to afford a way to measure nonlinear circular birefringences and two-photon circular dichroism. The authors estimated upper limits for the chiral modulations of nonlinear optic effects (the relative difference between the values of a nonlinear coefficient for the left- and right-handed circularly polarized light) that their techniques should be able to detect. In particular, such an upper limit for $\Delta\delta^{TPCD}/\bar{\delta}$, relevant for TPCD, is placed at $\approx 3 \times 10^{-3}$. Moreover, rather recently Li and co-workers[73] have performed studies of gas-phase and solution linear and nonlinear circular dichroism of R-(+)-3-methylcyclopentanone, involving measurements of $(2 + 1)$ resonance-enhanced multiphoton ionization circular dichroism, a process involving a TPCD step.

The large response is attributed to the unique combination of chirality and electron delocalization. Comparison with electronic circular dichroism (ECD) and two-photon absorption (TPA) shows that the three effects exhibit complementary features for unravelling the molecular structures. From an analysis of the frontier orbitals mostly involved in the one−electron excitation vectors, the largest TPCD response of tetramethoxy-bisquinone-dithia-[7]-helicene has been attributed to the charge-transfer character of the excited state, like for the parent TPA effect. The simulated ECD spectral characteristics have further been found to be in good agreement with experimental data, including the fact that the first low-energy dominant Cotton band is negative for (M)-helicenes. On the other hand, for the same handedness, the first dominant TPCD band is positive and mostly described by the magnetic dipole terms rather than by the quadrupole term.

Linear and in particular nonlinear spectroscopic properties as those discussed here, multiphoton absorption and dichroism, involving mixed electric and magnetic transitions, are demanding quantities. Their computational analysis requires care in the choice of approximations, adequate basis sets, an account for the inherent origin dependence of magnetic properties in approximate calculations, and, last but not least, caution in the use of functionals when resorting to DFT. The basis sets employed here are quite reasonable for the rather extended systems studied, and we employ origin independent approaches when needed. We have reasons to believe therefore that the major limitation of the present work might reside in the choice of the exchange correlation (XC) functional, which, in spite of its vast popularity and rather good performance in studies of other mixed electric-magnetic frequency dependent high order properties,[74,75] might be not completely adequate when delocalization effects or charge-transfer excitations become important, as they are proven to be here. It must be noted that several XC functionals, including B3LYP, have been shown to reproduce satisfactorily the ECD (and UV) spectra of helicenes, which might also be affected by the limitations of the functionals to treat long-range effects. Also, the drawbacks observed in DFT with conventional XC functionals are often associated with systems that are far more extended in space than those studied here, or far more conjugated, as polyacetylene and polydiacetylene chains. In recent times it was shown that the Coulomb Attenuating Method B3LYP (CamB3LYP) functional[76] may give good performance when dealing with two-photon absorption.[77] Nevertheless, ongoing studies carried out within our group along these lines on other systems lead us to believe that a different and more proper choice of functional, for instance in the direction of including long-range effects, might improve the agreement between theory and experiment on the position of the absorption peaks and influence the general features of our absorption and dichroism spectra, all the more for higher order processes. However, it should not be able disprove our evidence on the strong responses exhibited by the helicenes studied here.

Acknowledgment. This work has been supported by the European Research and Training Network "Understanding Nanomaterials from a Quantum Perspective" (NANOQUANT), contract No. MRTN-CT-2003-506842. B.C. thanks the FNRS for his Research director position.

References

(1) Martin, R. H. *Angew. Chem., Int. Ed.* **1974**, *13*, 649.

(2) Newman, M. S.; Lutz, W. B.; Lednicer, D. *J. Am. Chem. Soc.* **1955**, *77*, 3420.

(3) Groen, M. B.; Wynberg, H. *J. Am. Chem. Soc.* **1971**, *93*, 2968.

(4) Groen, M. B.; Schadenberg, H.; Wynberg, H. *J. Org. Chem.* **1971**, *36*, 2797.

(5) Yamada, K. I.; Tanaka, H.; Nakagawa, H.; Ogashiwa, S.; Kawazura, H. *Bull. Chem. Soc. Jpn.* **1982**, *55*, 500.

(6) Katz, T. J.; Liu, L.; Willmore, N. D.; Fox, J. M.; Rheingold, A. L.; Shi, S.; Nuckolls, C.; Rickman, B. H. *J. Am. Chem. Soc.* **1997**, *119*, 10054.

(7) Grimme, S.; Harren, J.; Sobanski, A.; Vögtle, F. *Eur. J. Org. Chem.* **1998**, 1491.

(8) Nuckolls, C.; Katz, T. J. *J. Am. Chem. Soc.* **1998**, *120*, 9541.

(9) Rajca, A.; Wang, H.; Pink, M.; Rajca, S. *Angew. Chem., Int. Ed.* **2000**, *39*, 4481.

(10) Phillips, K. E. S.; Katz, T. J.; Jockusch, S.; Lovinger, A.; Turro, N. *J. Am. Chem. Soc.* **2001**, *123*, 11899.

(11) Tanaka, K.; Osuga, H.; Kitahara, Y. *J. Org. Chem.* **2002**, *67*, 1795.

(12) Maiorana, S.; Papagni, A.; Licandro, E.; Annunziata, R.; Paravidino, P.; Perdicchia, D.; Giannini, C.; Bencini, M.; Clays, K.; Persoons, A. *Tetrahedron* **2003**, *59*, 6481.

(13) Field, J. E.; Hill, T. J.; Venkataraman, D. *J. Org. Chem.* **2003**, *68*, 6071.

(14) Rajca, A.; Miyasaka, M.; Pink, M.; Wang, H.; Rajca, S. *J. Am. Chem. Soc.* **2004**, *126*, 15211.

(15) Baldoli, C.; Bossi, A.; Giannini, C.; Licandro, E.; Maiorana, S.; Perdicchia, D. *Synlett* **2005**, 1137.

(16) Bazzini, C.; Brovelli, S.; Caronna, T.; Gambarotti, C.; Giannone, M.; Macchi, P.; Meinardi, F.; Mele, A.; Panzeri, W.; Recupero, F.; Sironi, A.; Tubino, R. *Eur. J. Org. Chem.* **2005**, 1247.

(17) Collins, S. K.; Grandbois, A.; Vachon, M. P.; Côté, J. *Angew. Chem., Int. Ed.* **2006**, *45*, 2923.

(18) Abbate, S.; Bazzini, C.; Caronna, T.; Fontana, F.; Gambarotti, C.; Gangemi, F.; Longhi, G.; Mele, A.; Sora, I. N.; Panzeri, W. *Tetrahedron* **2006**, *62*, 139.

(19) Wigglesworth, T. J.; Sud, D.; Norsten, T. B.; Lekhi, V. S.; Branda, N. R. *J. Am. Chem. Soc.* **2005**, *127*, 7272.

(20) Reetz, M. T.; Sostmann, S. *Tetrahedron* **2001**, *55*, 2515.

(21) Field, J. E.; Muller, G.; Riehl, J. P.; Venkataraman, D. *J. Am. Chem. Soc.* **2005**, *125*, 11808.

(22) Hassey, R.; Swain, E. J.; Hammer, N. I.; Venkataraman, D.; Barnes, M. D. *Science* **2006**, *314*, 1437.

(23) Verbiest, T.; Van Elsocht, S.; Kauranen, M.; Hellemans, L.; Snauwaert, J.; Nuckolls, C.; Katz, T. J.; Persoons, A. *Science* **1998**, *282*, 913.

(24) Verbiest, T.; Sioncke, S.; Persoons, A.; Vylicky, L.; Katz, T. J. *Angew. Chem., Int. Ed.* **2002**, *41*, 3882.

(25) Buss, V.; Kolster, K. *Chem. Phys.* **1996**, *203*, 309.

(26) Schulman, J. M.; Disch, R. L. *J. Phys. Chem. A* **1999**, *103*, 6669.

(27) Furche, F.; Ahlrichs, R.; Wacksmann, C.; Weber, E.; Sobanski, A.; Vögtle, F.; Grimme, S. *J. Am. Chem. Soc.* **2000**, *122*, 1717.

(28) Autschbach, J.; Ziegler, T.; van Gisbergen, S. J. A.; Baerends, E. J. *J. Chem. Phys.* **2002**, *116*, 6930.

(29) Spassova, M.; Asselberghs, I.; Verbiest, T.; Clays, K.; Botek, E.; Champagne, B. *Chem. Phys. Lett.* **2007**, *439*, 213.

(30) Daul, C. A.; Ciofini, I.; Weber, V. *Int. J. Quantum Chem.* **2003**, *91*, 297.

(31) Botek, E.; Champagne, B.; Turki, M.; André, J. M. *J. Chem. Phys.* **2004**, *120*, 2042.

(32) Champagne, B.; André, J. M.; Botek, E.; Licandro, E.; Maiorana, S.; Bossi, A.; Clays, K.; Persoons, A. *Chem. Phys. Chem* **2005**, *5*, 1438.

(33) Botek, E.; Spassova, M.; Champagne, B.; Asselberghs, I.; Persoons, A.; Clays, K. *Chem. Phys. Lett.* **2005**, *412*, 274.

(34) Botek, E.; Spassova, M.; Champagne, B.; Asselberghs, I.; Persoons, A.; Clays, K. *Chem. Phys. Lett.* **2006**, *417*, 282 (Erratum).

(35) Barron, L. D. *Molecular light scattering and optical activity*; Cambridge University Press: Cambridge, 2004.

(36) Hug, W.; Hangartner, G. *J. Raman Spectrosc.* **1999**, *30*, 841.

(37) Pecul, M.; Rizzo, A.; Leszczynski, J. *J. Phys. Chem. A* **2002**, *106*, 11008.

(38) Hug, W.; Haesler, J. *Int. J. Quantum Chem.* **2005**, *104*, 695.

(39) Herrmann, C.; Ruud, K.; Reiher, M. *ChemPhysChem* **2006**, *7*, 7189.

(40) Tinoco, I., Jr. *J. Chem. Phys.* **1975**, *62*, 1006.

(41) Jansík, B.; Rizzo, A.; Ågren, H. *Chem. Phys. Lett.* **2005**, *414*, 461.

(42) Rizzo, A.; Jansík, B.; Bondo Pedersen, T.; Ågren, H. *J. Chem. Phys.* **2006**, *125*, 064113.

(43) Jansík, B.; Rizzo, A.; Ågren, H. *J. Phys. Chem. B* **2007**, *111*, 446. Jansík, B.; Rizzo, A.; Ågren, H. *J. Phys. Chem. B* **2007**, *111*, 2409 (Erratum).

(44) Markowicz, P. P.; Samoc, M.; Cerne, J.; Prasad, P. N.; Pucci, A.; Ruggeri, G. *Opt. Expr.* **2004**, *12*, 5209.

(45) Wagnière, G. *J. Chem. Phys.* **1982**, *77*, 2786.

(46) Meath, W. J.; Power, E. A. *J. Phys. B.: At. Mol. Phys.* **1984**, *17*, 763.

(47) Meath, W. J.; Power, E. A. *Mol. Phys.* **1984**, *51*, 585.

(48) Meath, W. J.; Power, E. A. *J. Phys. B.: At. Mol. Phys.* **1987**, *20*, 1945.

(49) Meath, W. J.; Power, E. A. *J. Mod. Opt.* **1989**, *36*, 977.

(50) Power, E. A. *J. Chem. Phys.* **1975**, *63*, 1348.

(51) Andrews, D. L. *Chem. Phys.* **1976**, *16*, 419.

(52) Condon, E. U. *Rev. Mod. Phys.* **1937**, *55*, 2789.

(53) Craig, D. P.; Thirunamachandran, T. *Molecular Quantum Electrodynamics. An Introduction to Radiation Molecule Interaction*; Dover Publications, Inc.: Mineaol, NY, 1984.

(54) McClain, W. M. *Acc. Chem. Res.* **1974**, *7*, 129.

(55) Becke, A. D. *J. Chem. Phys.* **1993**, *98*, 5648.

(56) Becke, A. D. *Phys. Rev. **A*** **1988**, *38*, 3098.

(57) Lee, C.; Yang, W.; Parr, R. G. *Phys. Rev. B* **1988**, *37*, 785.

(58) Sałek, P.; Jonsson, D.; Vahtras, O.; Ågren, H. *J. Chem. Phys.* **2002**, *117*, 9630.

(59) Olsen, J.; Jørgensen, P. In *Modern Electronic Structure Theory, Part II*; Yarkony, D. R., Ed.; World Scientific: Singapore, 1995; Chapter 13, p 857.

(60) Dunning, T. H., Jr. *J. Chem. Phys.* **1989**, *90*, 1007.

(61) DALTON, a molecular electronic structure program, Release 2.0 (2005). See http://www.kjemi.uio.no/software/dalton/dalton.html.

(62) Albota, M.; Beljonne, D.; Brédas, J.-L.; Ehrlich, J. E.; Fu, J.-Y.; Heikal, A. A.; Hess, S. E.; Kogej, T.; Levin, M. D.; Marder, S. R.; McCord-Maughon, D.; Perry, J. W.; Röckel, H.; Rumi, M.; Subramaniam, G.; Webb, W. W.; Wu, X.-L.; Xu, C. *Science* **1998**, *281*, 1653.

(63) Bartholomew, G. P.; Rumi, M.; Pond, S. J. K.; Perry, J. W.; Tretiak, S.; Bazan, G. C. *J. Am. Chem. Soc.* **2004**, *126*, 11529.

(64) Ohta, K.; Kamada, K. *J. Chem. Phys.* **2006**, *124*, 124303.

(65) Norman, P.; Luo, Y.; Ågren, H. *J. Chem. Phys.* **1999**, *111*, 7758.

(66) Luo, Y.; Norman, P.; Macak, P.; Ågren, H. *J. Chem. Phys.* **2000**, *104*, 4718.

(67) Macak, P.; Luo, Y.; Norman, P.; Ågren, H. *J. Chem. Phys.* **2000**, *113*, 7062.

(68) Brickell, W. S.; Brown, A.; Kemp, C. M.; Mason, S. F. *J. Chem. Soc. A* **1971**, 756.

(69) Newman, M. S.; Darlak, R. S.; Tsai, L. *J. Am. Chem. Soc.* **1967**, *89*, 6191.

(70) Shen, Y. R. *The Principles of Nonlinear Optics*; Wiley-Interscience: Wiley Classics Library Ed.: New York, 2003.

(71) Meijer, E. W.; Havinga, E. E.; Rikken, G. L. J. A. *Phys. Rev. Lett.* **1990**, *65*, 37.

(72) Olsen, J.; Jørgensen, P. *J. Chem. Phys.* **1985**, *82*, 3235.

(73) Li, R.; Sullivan, R.; Al-Basheer, W.; Pagni, R. M.; Compton, R. N. *J. Chem. Phys.* **2006**, *125*, 144304.

(74) Baranowska, A.; Rizzo, A.; Jansík, B.; Coriani, S. *J. Chem. Phys.* **2006**, *125*, 054107.

(75) Jansík, B.; Rizzo, A.; Frediani, L.; Ruud, K.; Coriani, S. *J. Chem. Phys.* **2006**, *125*, 234105.

(76) Yanai, Y.; Tew, D. P.; Handy, N. C. *Chem. Phys. Lett.* **2004**, *393*, 51.

(77) Peach, M. J. G.; Helgaker, T.; Sałek, P.; Keal, T. W.; Lutnæs, O. B.; Tozer, D. J.; Handy, N. C. *Phys. Chem. Chem. Phys.* **2006**, *8*, 558.

CT700329A